RESEARCH ARTICLE

Human Mutation

OFFICIAL JOURNAL HGVS HUMAN GENOME VARIATION SOCIETY www.hgvs.org

Functional Characterization and Classification of Frequent Low-Density Lipoprotein Receptor Variants

Aitor Etxebarria,[1†] Asier Benito-Vicente,[1†] Lourdes Palacios,[2] Marianne Stef,[2] Ana Cenarro,[3] Fernando Civeira,[3] Helena Ostolaza,[1] and Cesar Martin[1*]

[1]*Unidad de Biofísica (CSIC, UPV/EHU) and Departamento de Bioquímica, Universidad del País Vasco, Bilbao 48080, Spain;* [2]*Progenika Biopharma, Grifols, Derio, Spain;* [3]*Unidad de Lípidos and Laboratorio de Investigación Molecular, Hospital Universitario Miguel Servet, Instituto Aragonés de Ciencias de la Salud (IACS), Zaragoza, Spain*

Communicated by George P. Patrinos

Received 20 June 2014; accepted revised manuscript 24 October 2014.
Published online 6 November 2014 in Wiley Online Library (www.wiley.com/humanmutation). DOI: 10.1002/humu.22721

ABSTRACT: Familial hypercholesterolemia (FH) is an autosomal-dominant disorder mostly caused by mutations in the low-density lipoprotein receptor (LDLR) gene leading to increased risk for premature cardiovascular diseases. According to functional studies, *LDLR* mutations may be classified into five classes. The main objective of this study was to characterize seven *LDLR* variants previously detected in FH patients. Analysis by flow cytometry and confocal microscopy of LDLR activity demonstrate that all the studied variants are pathogenic. Among the mutations located in β-propeller, p.Trp577Gly and p.Ile624del were classified as class 2, whereas p.Arg416Trp and p.Thr454Asn as class 5. p.Phe800Glyfs*129 (located in the cytoplasmic domain), p.Cys155Tyr (located in the binding domain), and p.Asn825Lys (inside FxNPxY motif) were classified as class 2, 3, and 4, respectively. The results also show that LDLR activity of these class 4 and 5 variants is not completely abolished, showing a milder phenotype. We have also determined that statin response is more efficient lowering total cholesterol in heterozygous patients carrying p.Ile624del (class 2) compared with p.Arg416Trp and p.Thr454Asn (class 5) variants. In conclusion, these findings emphasize the importance of characterizing *LDLR* pathogenic variants to provide an indisputable FH diagnosis and to gain insight into the statin response depending on the LDLR class mutation.
Hum Mutat 36:129–141, 2015. © 2014 Wiley Periodicals, Inc.

KEY WORDS: LDRL; mutations; familial hypercholesterolemia; statins; mutation class defect

Introduction

Familial hypercholesterolemia (FH; MIM #143890) is a common autosomal-dominant genetic disorder characterized by high plasma levels of low-density lipoprotein-cholesterol (LDL-c). FH is mainly caused by mutations in the genes coding for the LDL receptor (LDLR; MIM #606945) [Brown and Goldstein, 1986], apolipoprotein B (APOB; MIM #107730) [Innerarity et al., 1990], and proprotein convertase subtilisin/kexin 9 (PCSK9; MIM #607786) [Abifadel et al., 2003], with a frequency of 1:500 individuals in its heterozygous form [Goldstein and Brown, 2001; Soutar and Naoumova, 2007]. Diagnosis of FH is mainly based on lipid levels (usually LDL >190 mg/dl) in untreated adults, clinical signs, family history of dyslipidemia, and/or premature coronary heart disease (CHD). The clinical phenotype is variable, showing high levels of total cholesterol and LDL-c in the plasma and usually, presence of arcus corneae, xanthelasmas, xanthomas, and premature atherosclerosis [Hobbs et al., 1992]. However, such clinical signs are rarely present in children carrying pathogenic mutations and therefore the clinical diagnosis may miss a considerable proportion of FH-positive pediatric patients in whom the phenotype has not already developed.

The majority of FH cases are related to mutations occurring within *LDLR*. The LDLR in its mature form is a glycosylated protein with a molecular mass of 160 kDa [Tolleshaug et al., 1982] located in the cell surface where it mediates the uptake of lipoprotein particles, mainly LDL. To date, more than 1,300 different mutations in the LDLR gene have been identified worldwide [Leigh et al., 2008]. LDLR gene, located on chromosome 19p, comprises 18 exons, introns, and the promoter region [Yamamoto et al., 1984; Sudhof et al., 1985]. According to the nature and location of the mutations within the *LDLR* and to the phenotypic effects on the protein, mutations have been divided into five different classes [Hobbs et al., 1992]: Class 1: no detectable LDLR synthesis; Class 2: defective LDLR transport; Class 3: impaired LDL to LDLR binding; Class 4: no LDLR/LDL internalization due to defective clustering in clathrin coated pits; and Class 5: no LDLR recycling.

The Class of *LDLR* mutation has been associated with different phenotype [Hoeg, 1993; Kotze et al., 1993; Gudnason and Humphries, 1999], response to statins [Leren and Hjermann, 1995; Vuorio et al., 1995], and risk of premature CHD [Vohl et al., 2002]. It has been previously shown that statin treatment of heterozygous patients carrying Class 2 and Class 5 mutations exhibit higher percentage decrease in LDL-c compared with patients carrying Class 1, Class 3, or Class 4 mutations [Chaves et al., 2001; Miltiadous et al., 2006]. However, the efficacy of statins treatment is highly variable and several genetic and environmental factors can contribute to

Additional Supporting Information may be found in the online version of this article.

[†]These authors equally contributed to this work.

*Correspondence to: Cesar Martin, Unidad de Biofísica (CSIC, UPV/EHU) and Departamento de Bioquímica, Universidad del País Vasco, Apdo 644, Bilbao 48080, Spain. E-mail: cesar.martin@ehu.es

Contract grant sponsors: Spanish Ministry of Economy and Competitiveness, Programa INNPACTO (grant No IPT-2011-0817-010000), Spanish Ministerio de Ciencia y Tecnología (Project BFU 2012-36241), and FIS PI12/01087).

Table 1. Characteristics of *LDLR* Variants Included in the Study

	Location	cDNA (HGVS)	Protein (HGVS)	LDLR domain	Reference
Positive controls	Exons 3 and 4	c.191-?_694+?del	p.Leu64_Ala232delinsSer	Ligand binding	[Marduel et al., 2010; Etxebarria et al., 2012]
	Exon 3	c.261G>A	p.Trp87*	Ligand binding	[Tosi et al., 2007]
Single-nucleotide variants	Exon 4	c.464G>A	p.Cys155Tyr	Ligand binding	[Marduel et al., 2010]
	Exon 9	c.1246C>T	p.Arg416Trp	β-propeller	[Leren et al., 1997; Bertolini et al., 2013]
	Exon 10	c.1361C>A	p.Thr454Asn	β-propeller	[Mozas et al., 2004]
	Exon 12	c.1729T>G	p.Trp577Gly	β-propeller	[Marduel et al., 2010]
	Exon 17	c.2475C>A	p.Asn825Lys	FxNPxY motif	[Jensen et al., 1999]
	Exon 13	c.1871_1873delTCA	p.Ile624del	β-propeller	[Chmara et al., 2010; Bertolini et al., 2013]
	Exon 17	c.2399_2403delTCTTC insGGGT	p.Phe800Glyfs*129	Cytoplasmic tail	[Mozas et al., 2004]

Nucleotide numbering uses +1 as the A of the ATG translation initiation codon in RefSeq NM_000527.3, with the initiation codon as codon 1. Furthermore, amino acid variants follow the standard nomenclature with the initiating methionine given as number one, rather than the historical numbering from the first residue of the mature peptide.

treatment response. Therefore, the mechanism and efficacy of statin induced LDL-c lowering related to the class type mutation causing FH remains controversial [Choumerianou and Dedoussis, 2005]. Knowledge of the phenotype of patients carrying *LDLR* mutations and response to statins of the different classes of pathogenic LDLR could favor a more appropriate treatment and better prognosis of FH.

In this study, we have analyzed seven *LDLR* variants, previously found in FH patients but without a functional characterization or Class assignment. The obtained data confirm the pathogenicity of the seven variants analyzed and they have been classified according LDLR class mutation. We have also analyzed the statin response of heterozygous patients carrying Class 2 and Class 5 variants. We have found similar lipid phenotype in heterozygous patients carrying Class 2 variant or Class 5. However, the obtained results in the homozygous situation, mimicked by CHO-*ldl*A7 transfected cells, show that phenotype of patients carriying Class 2 variants is more severe than the phenotype of Class 5 variants.

Materials and Methods

Selection of Variants

The seven *LDLR* variants were previously found in FH patients, being common in Spanish population and their selection was based on their location in *LDLR*. To cover the first criteria, we selected variants previously described by other authors in FH patients (www.ucl.ac.uk/ldlr/LOVDv.1.1.0/ and www.umd.be/LDLR/) and that have also been found in at least four FH index cases by LIPOchip® platform [Palacios et al., 2012] or by SEQPRO LIPO RS® platform in Progenika Biopharma (Derio, Spain), both platforms with the CE mark. Four of the selected variants are located in the β-propeller: p.Arg416Trp (c.1246C>T), p.Thr454Asn (c.1361C>A), p.Trp577Gly (c.1729T>G), and p.Ile624del (c.1871_1873delTCA). One variant is in the binding domain affecting a cysteine residue: p.Cys155Tyr (c.464G>A) and another one changes the FxNPxY motif, p.Asn825lys (c.2475C>A). The last variant, p.Phe800Glyfs*129 (c.2399_2403delTCTTCinsGGGT), is a frameshift causing a stop codon that does not fulfill requirements to be degraded by the nonsense-mediated decay system [Holla et al., 2009], and it is predicted to result in a completely different cytoplasmic tail. Nucleotide numbering uses +1 as the A of the ATG translation initiation codon in the reference sequence NM_000527.3, with the initiation codon as codon 1. Furthermore, amino acid variants follow the standard nomenclature with the initiating methionine given as number one, rather than the historical numbering from the first residue of the mature peptide. The characteristics of selected variants are compiled in Table 1.

Cell Culture and Transfection

LDLR-deficient Chinese hamster ovary (CHO) cell line *ldlA7* (CHO-*ldlA7*) (kindly provided by Dr. Monty Krieger, Massachusetts Institute of Technology, Cambridge, MA) was cultured in Ham's F-12 medium supplemented with 5% FBS, 2 mM L-glutamine, 100 units/ml penicillin, and 100 μg/ml streptomycin. CHO-*ldlA7* cells were plated into six- or 24-well culture plates, and transfected with plasmids carrying the *LDLR* mutations using Lipofectamine® LTX and Plus™ Reagent (Invitrogen, Life Technologies, Alcobendas, Spain) according to the manufacturer's instructions. Transfected cells were maintained in culture during 48 hr to achieve maximal LDLR expression.

Western Blot Analysis

Cell lysates were prepared, protein concentration determined, and fractionated by electrophoresis on nonreducing 8.5% SDS-PAGE for semiquantitative immunoblotting. Membranes were immunostained with rabbit polyclonal anti-LDLR antibody (1:2,000) (Progen Biotechnik GmbH, Heidelberg, Germany) for 16 hr at 4°C and anti-GAPDH antibody (1:1,000) (Nordic Biosite, Täby, Sweden) for 1 hr at room temperature and counterstained with a horseradish peroxidase-conjugated antirabbit antibody (GE Healthcare, Little Chalfont, UK). The signals were developed using SuperSignal West Dura Extended Substrate (Pierce Biotechnology, Rockford, IL). ChemiDoc XRS (Bio-Rad, Hercules, CA) was used to detect the signals, and Quantity One Basic 4.4.0 software (Bio-Rad) was used to quantify band intensities. The concentrations of the antibodies were optimized to achieve low background and a linear dose-dependent increase in signal intensity. The relative LDLR expression for the different constructs was calculated as the ratio between the sum of band intensities corresponding to the mature and precursor form of LDLR protein to that of GAPDH.

Quantification of LDLR Activity by Flow Cytometry

Transfected CHO-*ldlA7* cells were grown in 24-well culture plates. Forty-eight hours after transfection, cells were incubated for 4 hr, at 37°C and at 4°C with 20 μg/ml FITC–LDL to determine LDLR activity or LDL–LDLR binding, respectively. After incubation with FITC–LDL, CHO-*ldlA7* cells were washed twice in PBS-1% BSA, fixed on 4% formaldehyde for 10 min and washed again twice with PBS-1% BSA. To determine the amount of internalized LDL, Trypan blue solution (Sigma–Aldrich, Steinheim, Germany) was added to a final concentration of 0.2% directly to the samples, eliminating the extracellular signal due to the noninternalized LDL–LDLR complexes. Fluorescence intensities were measured by FACS, in a Facscalibur flow cytometer according to the manufacturer instructions as previously described [Etxebarria et al., 2012]. For each sample, fluorescence of 10,000 events was acquired for data analysis. All measurements were performed at least in triplicate.

Quantification of LDLR Expression by Flow Cytometry

To determine LDLR cell surface expression by FACS, transfected CHO-*ldlA7* cells grown during 48 hr were incubated with a mouse primary antibody anti-LDLR (1:100; 2.5 mg/l; Progen Biotechnik GmbH) for 1 hr, at room temperature, then washed twice with PBS-1% BSA and incubated with secondary antibody Alexa Fluor 488-conjugated goat antimouse IgG (1:100; Molecular Probes). For each sample, fluorescence of 10,000 events was acquired for data analysis. All measurements were performed at least in triplicate.

Confocal Laser Scanning Microscopy

Confocal laser scanning microscopy was used to analyze LDL–LDLR binding, uptake, expression of LDLR, and colocalization with clathrin, lysosomes, or endoplasmic reticulum (ER). Briefly, cells were plated in coverslips and then transfected with the *LDLR* containing plasmids and cultured for 48 hr, at 37°C in 5% CO_2. Then, the medium was removed and coverslips washed twice with PBS-1% BSA. For these studies, nonlabeled lipoproteins (20 μg/ml LDL) were added and cells were incubated at 37°C for additional 4 hr. Cells were fixed with 4% paraformaldehyde during 10 min and washed three times with PBS-1% BSA and permeabilized with 1% TritonX-100 for 30 min at room temperature. Samples were then washed and blocked in PBS-10% FBS for 1 hr and washed in PBS-1% BSA three times. Then, samples were incubated with the appropriate primary antibodies for 16 hr at 4°C followed by incubation with the appropriate fluorescent secondary antibodies. To visualize clathrin colocalization with LDLR, cells were also transfected with a plasmid carrying clathrin-DsRed. To determine LDLR and LDL colocalization with lysosomes, LDL was labeled with vibrant DiI. Coverslips were mounted on a glass slide and samples were visualized using a confocal microscope (Olympus IX 81, Tokyo, Japan) with sequential excitation and capture image acquisition with a digital camera (Axiocam NRc5; Zeiss, Jena, Germany). Images were processed with Fluoview v50 software (Olympus, Miami, FL). Image analysis to quantify the fluorescence intensities was accomplished using the public domain software ImageJ (available at http://rsb.info.nih.gov/ij) running on a standard PC.

LDL–LDLR Binding at Different pH

CHO-*ldlA7* cells were transfected with plasmids carrying the *LDLR* mutations as described before, and then incubated with 20 μg/ml of LDL–FITC for 30 min in a 0.4-M sucrose supplemented Ham's medium at different pH. Then, cells were washed three times to remove the unbound LDL, fixed with 4% paraformaldehyde for 10 min, and washed again with Ham's medium at its corresponding pH in each case. Bound LDL–FITC was determined as described before.

Subjects to Study Response to Statin Therapy

Subjects with clinical diagnosis of FH and the *LDLR* variants: p.Thr454Asn, p.Arg416Trp, and p.Ile624del were selected from the Lipid Clinic of the Hospital Universitario Miguel Servet (Zaragoza, Spain). Nine subjects with p.Thr454Asn variant, three subjects with p.Arg416Trp variant, and four subjects with p.Ile624del variant were studied. Informed consent was obtained from all subjects and by Comité Ético de Investigación Clínica de Aragón (CEICA). Procedures were in accordance with the Helsinki Declaration of 1975, as revised in 2000.

Further details concerning the in silico-predicted effect of molecular event on LDLR, conservation analysis, statistical analysis, site-directed mutagenesis, lipoprotein isolation, lipoprotein labeling, serum lipid determinations, isolation and culture of T-lymphocytes, quantification of LDLR activity by flow cytometry in human lymphocytes, and quantification of LDLR expression by flow cytometry in human lymphocytes are provided in the Supporting Information. Supplementary figures showing LDLR activity in lymphocytes carrying wild-type (wt) LDLR, and Ex3_4del or p.Arg416Thr variants and the effect of simvastatin on LDL-c decrease in Class 2 and Class 5 LDLR heterozygous patients is shown in Supporting Information.

Results

In silico Analysis

The results obtained by different software packages are presented in Table 2. All the variants except p.Thr454Asn were classified as pathogenic by the majority of the prediction programs. No splicing defects were predicted for any of the studied variants.

Expression of LDLR Variants in CHO-*ldlA7* Cells

CHO-*ldl*A7 cells were transfected with plasmids carrying the different mutations and LDLR expression was assayed by immunoblotting as described in *Materials and Methods*. As shown in Figure 1, all the studied LDLR variants show similar protein expression 48 hr after transfection. The relative band intensity of LDLR protein expressed in the different cell lines was calculated as the ratio between the sum of 160 and 120 kDa bands to that of GADPH and resulted not statistically significant among the different variants. In wt *LDLR*-transfected cells, two bands were detected, one corresponding to the mature form of the receptor (apparent molecular weight 160 kDa) (Fig. 1, lanes 1 and 5); and another faint band corresponding to the short-lived precursor form (apparent molecular weight 120 kDa). For variants p.Phe800Glyfs*129, p.Ile624del, and p.Trp577Gly, only one band was detected, corresponding to the precursor form of the receptor protein (Fig. 1, lanes 2–4). For variants p.Cys155Tyr, p.Asn825Lys, p.Arg416Trp, and p.Thr454Asn, the band signal was similar to the wt LDLR (Fig. 1, lanes 6–9).

Table 2. Description of the Studied Variants, Conservation, and In Silico Predictions

				Pathogenicity prediction			
cDNA (HGVS)	Protein (HGVS)	Nucleotide conservation	Amino acid conservation	Align GVGD[a]	SIFT	Polyphen-2	Mutation taster 2
c.1246C>T	p.Arg416Trp	0.91	0.91	C35	Deleterious (score 0)	Probably damaging (1)	Disease causing (*P*: 1.0)
c.1871_1873delTCA	p.Ile624del	NA	0.70	NA	Deleterious	NA	Polymorphism (*P*: 0.86)
c.2475C>A	p.Asn825Lys	0.85	1.00	C65	Deleterious (score 0)	Probably damaging (1)	Disease causing (*P*: 1.0)
c.464G>A	p.Cys155Tyr	0.97	0.97	C65	Deleterious (score 0)	Probably damaging (1)	Disease causing (*P*: 1.0)
c.1361C>A	p.Thr454Asn	0.94	0.53	C0	Deleterious (score 0.04)	Benign (0.138)	Polymorphism (*P*: 0.999)
c.2399_2403del TCTTCinsGGGT	p.Phe800Glyfs*129	NA	NA	NA	Deleterious	NA	Disease causing (*P*: 1.0)
c.1729T>G	p.Trp577Gly	1.00	1.00	C65	Deleterious (score 0.04)	Probably damaging (1)	Disease causing (*P*: 1.0)

[a]Score values are from C0 (not pathogenic) to C65 (pathogenic).
Details on variant in silico prediction methods provided in Supp. Methods.
NA, nonapplicable.

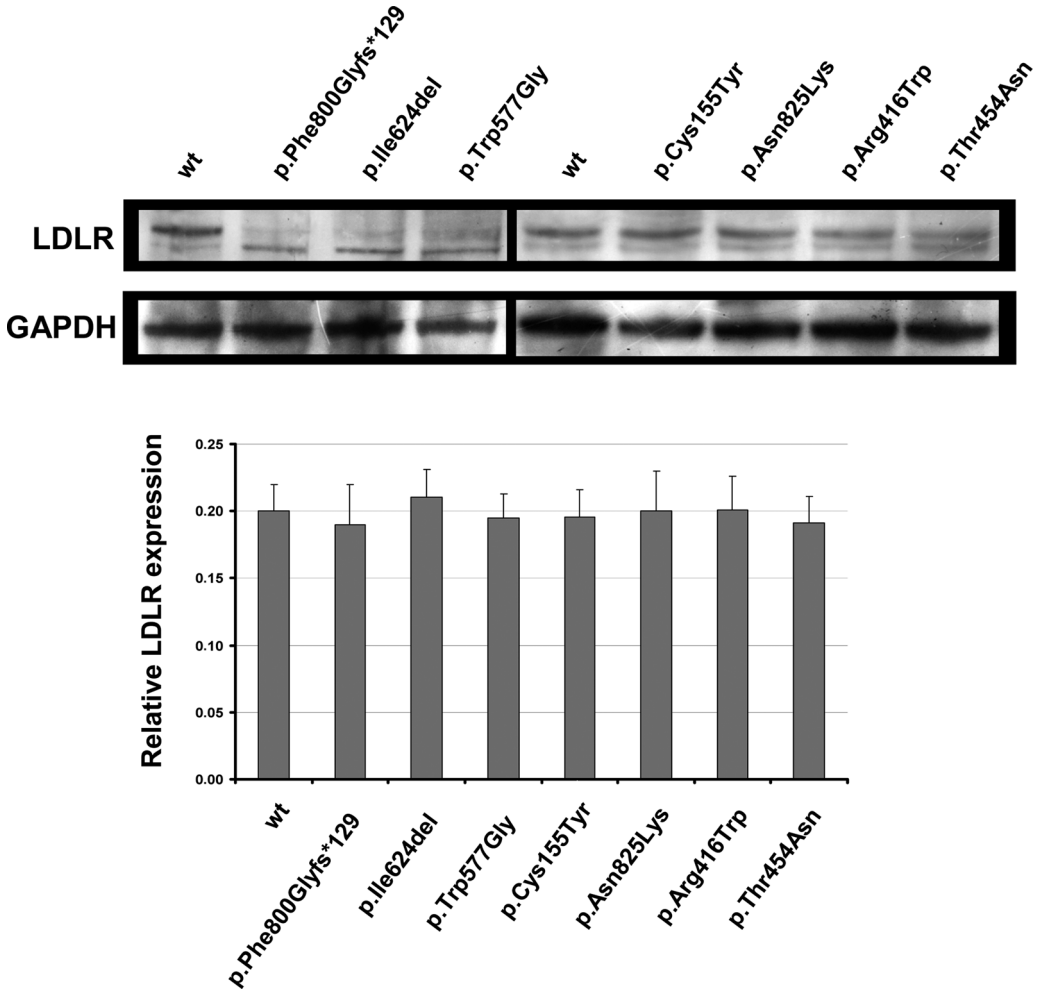

Figure 1. Expression of wt LDLR and LDLR variants in CHO-*ldlA7* transfected cells. Cells were transfected with the corresponding plasmids carrying the mutations of interest, LDLR was overexpressed for 48 hr, and then cells were lysed and analyzed by Western blot. Whole cell extracts (20 μg) were fractioned in nonreducing 8.5% SDS-PAGE, transferred onto nitrocellulose membranes for incubation with a rabbit polyclonal anti-hLDLR antibody and detected by chemioluminiscence as described in *Materials and Methods* section. The relative band intensity of LDLR protein expressed in the different cell lines was calculated as the ratio between the sum of 160 and 120 kDa bands to that of GADPH. A representative experiment from three independently performed assays is shown in upper panel. Levels of significance were determined by a two-tailed Student's *t*-test, and a confidence level of greater than 95% ($P < 0.05$) was used to establish statistical significance. No statistically significant differences were found among the LDLR expression.

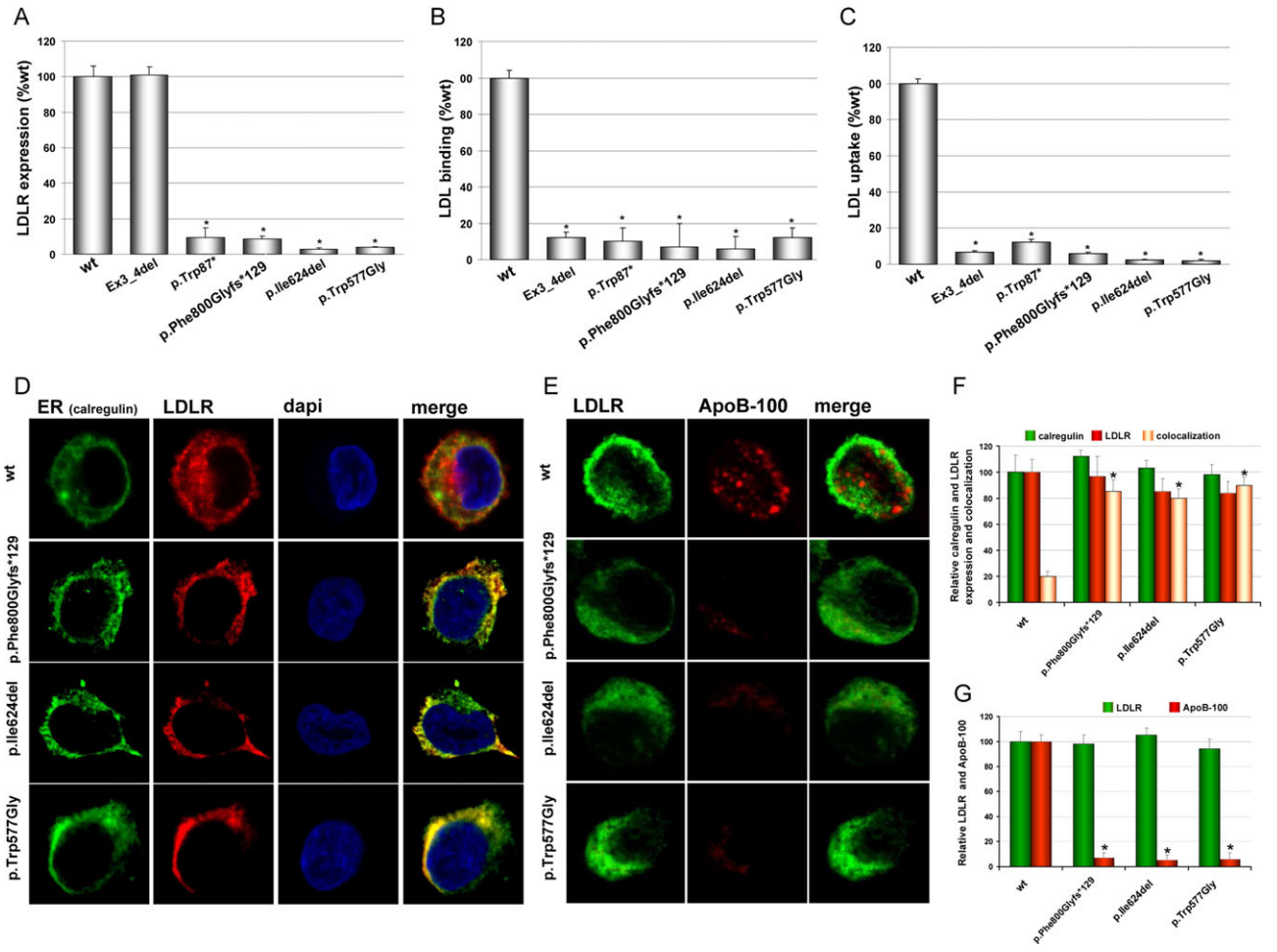

Figure 2. Functional characterization of p.Trp577Gly; p.Ile624del and p.Phe800Glyfs*129 LDLR variants. **A**: LDLR expression at cellular membrane. **B**: LDL-LDLR binding after 4 hr incubation at 4°C **C**: LDL internalization after 4 hr incubation at 37°C. **D**: Subcellular colocalization of p.Trp577Gly, p.Ile624del, and p.Phe800Glyfs*129 LDLR variants with the ER-specific marker calregulin. **E**: Localization of LDLR and LDL after 4 hr incubation at 37°C. **F**: Relative LDLR and calregulin expression and colocalization. **G**: Relative amount of LDLR and LDL. For flow cytometry determinations, 10,000 cells were acquired in a Facscalibur, and values of LDL uptake, binding, and LDLR expression were calculated as described in *Materials and Methods*. Confocal analysis of the LDLR colocalization with ER was performed in wt and LDLR variants. Transfected cells were immunostained as described in *Materials and Methods*. Image analysis to quantify the fluorescence intensities of the confocal images was performed with ImageJ. The values in A–C represent the mean of triplicate determinations ($n = 3$); error bars represent ± SD. $^*P < 0.001$ compared with the wt using a Student's *t*-test. The images in D and E show a representative individual cell. The histograms in F and G represent the mean ± SD ($n = 30$ cells) of the confocal images quantification, $^*P < 0.001$ compared with the wt using a Student's *t*-test.

Class 2 Variants: p.Trp577Gly; p.Ile624del; p.Phe800Glyfs*129

According to in silico analysis, the three variants would be pathogenic (Table 2). The translation product of p.Phe800Glyfs*129 variant is predicted to be a mature LDLR protein of 908 amino acids instead of 839 amino acids in which the cytoplasmic tail would have a totally different sequence as compared with the wt. To determine LDLR activity of these variants, LDLR expression and LDL binding and uptake were analyzed in CHO-*ldlA7* transfected cells by FACS as described in *Materials and Methods*. As an internal control of the assay, cells transfected with plasmids containing a null *LDLR* allele (p.Trp87*) or a *LDLR* harboring an in frame deletion of exons 3 and 4 (EX3_4del, p.L64S;S65_P105del) were used. According to functional assays performed in heterozygous patients [Etxebarria et al., 2012], p.Trp87* variant codifies a mRNA that does not express LDLR and EX3_4del variant codifies a LDLR that is normally expressed but unable to bind LDL. Figure 2A shows that cells carrying the vectors containing p.Trp577Gly; p.Ile624del and p.Phe800Glyfs*129 *LDLR* variants do not express LDL receptor at membrane surface compared with wt-transfected cells (wt: 100 ± 5.0; p.Trp577Gly: 3.6 ± 0.3; p.Ile624del: 2.7 ± 0.3; and p.Phe800Glyfs*129: 8.6 ± 1.3). Accordingly, LDL binding and LDL uptake by the transfected cells with p.Trp577Gly; p.Ile624del or p.Phe800Glyfs*129 LDLR variants are almost completely abolished (wt: 100 ± 4.2; p.Trp577Gly: 11.8 ± 4.2; p.Ile624del: 6.3 ± 6.2; and p.Phe800Glyfs*129: 7.2 ± 6.3 for binding; wt: 100 ± 2.7; p.Trp577Gly: 2.1 ± 0.6; p.Ile624del: 2.2 ± 0.4; and p.Phe800Glyfs*129: 5.9 ± 0.9 for uptake) (Fig. 2B and C). The results show that these three variants are pathogenic showing a near complete loss of LDLR expression at cellular membrane. To further analyze the class type defect produced by these variants, we studied by confocal microscopy if there was any cellular LDLR expression and in such case where do the LDLR localizes within the cell. Confocal images show that the three LDLR variants are expressed in transfected cells but they keep clearly retained in the ER as indicated by the high colocalization with calregulin, an ER marker

(Fig. 2D) and LDLR activities determined by confocal microscopy (Fig. 2E) confirm those obtained by FACS. Quantification of fluorescence associated intensities of confocal microscopy images is shown in Figure 2F and G. Taking into account the results obtained both by FACS and confocal microscopy, p.Trp577Gly; p.Ile624del or p.Phe800Glyfs*129 LDLR variants should be classified as Class 2a defective pathogenic variants.

Class 3 Variant: p.Cys155Tyr

p.Cys155Tyr variant, frequently found in Spanish FH patients, is located in the ligand-binding domain and is involved in a disulfide bond. Both nucleotide and amino acid are highly conserved among species and in silico analysis predicts this variant as pathogenic (Table 2). Therefore, we analyzed the functionality of this variant to corroborate the in silico prediction and to study the mutation class presenting by the cells expressing this LDLR variant. As shown in Figure 1, the expression of this LDLR variant is similar to the LDLR expressed in wt CHO-*ldlA7*-transfected cells (Fig. 1, lanes 1 and 5 wt, and lane 6 p.Cys155Tyr). We next studied by FACS and by confocal microscopy the activity of this LDLR variant. FACS analysis of LDLR expression showed that the receptor levels at membrane surface of this variant are similar to those present in the wt LDLR (wt: 100 ± 5.0; pCys155Tyr: 96.7 ± 2.5) (Fig. 3A). LDL binding and uptake determined by FACS show that pCys155Tyr LDLR variant does not bind LDL correctly (wt: 100 ± 4.2; pCys155Tyr: 15.4 ± 4.5) (Fig. 3B), and LDL internalization results almost completely abolished (wt: 100 ± 2.7; pCys155Tyr: 19.0 ± 1.6) (Fig. 3B). EX3_4del variant, in which the binding capacity is totally impaired, and p.Trp87* variant, which is a null allele, were used as internal controls. Here, a confocal microscopy analysis was conducted to confirm the results obtained by FACS. As shown in Figure 3D, p.Cys155Tyr variant is correctly expressed at cellular membrane, but it is not able to bind LDL. Quantification of fluorescence associated intensities of confocal microscopy images is shown in Figure 3E. The set of results obtained by different methodologies show that p.Cys155Tyr variant presents a defective ligand-binding activity, thus should be classified as Class 3 pathogenic variant.

Class 4 Variant: p.Asn825Lys

p.Asn825Lys variant substitutes the asparagine of the FxNPxP motif and it is expected to affect the internalization of the complex LDLR–LDL. Both nucleotide and amino acid are highly conserved among species and in silico analysis predicts this variant as pathogenic (Table 2). As shown in Figure 1, expression of p.Asn825Lys variant is similar to the wt expressed in LDLR in CHO-*ldlA7*-transfected cells (Fig. 1, lanes 1 and 5 wt, and lane 7 p.Asn825Lys). As shown in Figure 4A, LDLR expression determined by FACS at membrane surface is similar to that determined in the wt LDLR-transfected cells (wt: 100 ± 5.0; p.Asn825Lys: 86.7 ± 0.8). Consequently, we analyzed LDL binding and uptake to assess a possible defect of LDLR activity; thus, cells were incubated with FITC-labeled LDL as described in *Materials and Methods*. Results obtained in cells carrying p.Asn825Lys LDLR variant show that LDL/LDLR binding is not affected, being the FITC–LDL-associated fluorescence similar to the fluorescence determined in wt LDLR (wt: 100 ± 4.2; p.Asn825Lys: 93.5 ± 5.2) (Fig. 4B). However, when determining uptake efficiency, LDL internalization in p.Asn825Lys LDLR variant-transfected cells resulted in significantly diminished uptake compared with wt LDLR (wt: 100 ± 4.2; p.Asn825Lys: 56.7 ± 7.8) (Fig. 4C). The integrity of the FxNPxY sequence in the cytoplasmic tail of the LDLR is absolutely required for internalization [Davis et al., 1986; Chen et al., 1990]. Hence, confocal microscopy analysis of LDLR localization after LDL binding was conducted in cells transfected with wt LDLR or p.Asn825Lys LDLR variant to determine a possible defect in LDLR mobilization into clathrin-coated pits. The results shown in Figure 4D confirm that p.Asn825Lys does not bind correctly to clathrin after LDL binding, and in consequence, LDL internalization results significantly impaired (Fig. 4E). Quantification of fluorescence associated intensities of confocal microscopy images is shown in Figure 4F and G. These results sustain the classification of p.Asn825Lys LDLR variant as Class 4 pathogenic variant.

Class 5 Variants: p.Arg416Trp; p.Thr454Asn

p.Arg416Trp and p.Thr454Asn variants are located in the β-propeller. The p.Arg416Trp has been found in multiple FH patients worldwide and its association with FH has been demonstrated [Leren et al., 1997], but the mechanism affected is not known. p.Thr454Asn has only been described in Spanish patients [Mozas et al., 2004]. Amino acid conservation in p.Thr454Asn is lower (17/32) and the in silico analyses classify it as a nonpathogenic variant except for SIFT (Table 2). As shown in Figure 1 (lanes 1 and 5 wt, lanes 8 and 9 p.Arg416Trp and p.Thr454Asn, respectively), p.Arg416Trp and p.Thr454Asn LDLR variants do not seem to affect the expression of the receptor, resulting very similar to the wt LDLR expressed in CHO-*ldlA7*-transfected cells. FACS analysis of LDLR expression showed a significantly reduced receptor levels at membrane surface in both variants when compared with the wt LDLR expression (wt: 100 ± 5.0; p.Arg416Trp: 61.5 ± 5.3; p.Thr454Asn: 60.2 ± 7.6) (Fig. 5A). Then, LDL–LDLR binding and LDL uptake were analyzed as described before. Figure 5B and C shows that both binding activity and LDL internalization are significantly diminished in p.Arg416Trp and in p.Thr454Asn LDLR-transfected cells when compared with wt LDLR binding and internalization activities (wt: 100 ± 4.2; p.Arg416Trp: 53.2 ± 12.8; p.Thr454Asn: 63.9 ± 6.8 for binding and, wt: 100 ± 2.7; p.Arg416Trp: 58.6 ± 1.2; p.Thr454Asn: 63.9 ± 1.6 for LDL uptake). In a similar way, in heterozygous patient harboring p.Arg416Trp variant, LDLR expression levels and uptake efficiency were decreased when compared with wt LDLR (Supp. Fig. S1). The LDLR activities were determined in lymphocytes as described in Supp. Methods being wt: 100 ± 1.2; p.Arg416Trp: 71.5 ± 7.4 for LDLR expression and, wt: 100 ± 2.8; p.Arg416Trp: 42.5 ± 1.3 for LDL uptake. According to this phenotype, we analyzed LDLR expression and LDL–LDLR binding at different incubation times in the presence of LDL to figure out if the recycling process was affected. If this was the case, and as a consequence of a defective LDLR recycling, internalized LDL–LDLR complex would not dissociate in the endosome and LDLR would be thus degraded in the lysosomal compartment. The result of this defect would be a time-dependent progressive clearance of the LDLR from the cell surface and also a lower LDL uptake compared with a nondefective LDLR recycling in which the surface amount of LDLR remains at higher concentrations as a consequence of a correct recycling. Accordingly, cells transfected with wt *LDLR*, p.Arg416Trp, or p.Thr454Asn *LDLR* variants were incubated with LDL up to 2 hr. At different incubation times, LDLR expression and LDL uptake were determined as indicated in *Materials and Methods*. As shown in Figure 5D, LDLR expression resulted significantly diminished after 30 min of LDL addition in p.Arg416Trp variant and after 60 min in p.Thr454Asn LDLR variant. These results point out that LDLR recycling could be defective. Similarly, LDL uptake was determined in a time-dependent manner and as shown in Figure 5E, LDL

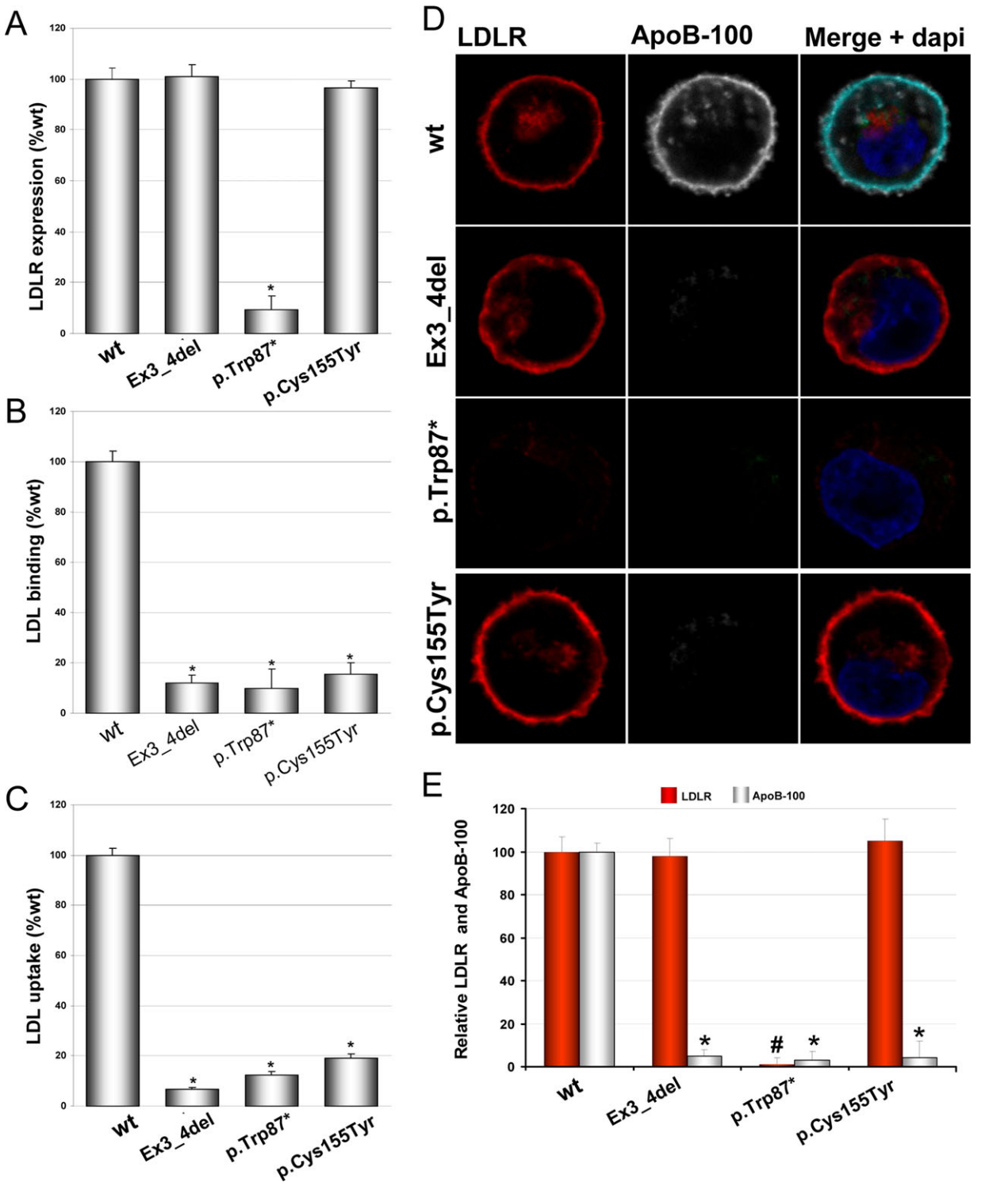

Figure 3. Functional characterization of p.Cys155Tyr LDLR variant. Quantification of: **A**: LDLR expression at membrane; **B**: LDL–LDLR binding after 4 h incubation at 4°C; **C**: LDL internalization after 4 h incubation at 37°C; **D**: localization of LDLR and LDL after 4 hr incubation at 37°C; and **E**: relative LDLR expression, and internalized, and bound LDL. For flow cytometry determinations, 10,000 cells were acquired in a Facscalibur and values of LDL uptake, binding, and LDLR expression were calculated as described in *Materials and Methods*. Transfected cells were immunostained as described in *Materials and Methods*. Image analysis to quantify the fluorescence intensities of the confocal images was performed with ImageJ. The values of FACS analysis represent the mean of triplicate determinations ($n = 3$); error bars represent ±SD. $^{*}P < 0.001$ compared with the wt using a Student's *t*-test. The confocal images show a representative individual cell. The histograms in E represent the mean ± SD ($n = 30$ cells) of the confocal images quantification, $^{\#}P < 0.001$ compared with the LDLR wt and $^{*}P < 0.001$ compared with ApoB-100 using a Student's *t*-test.

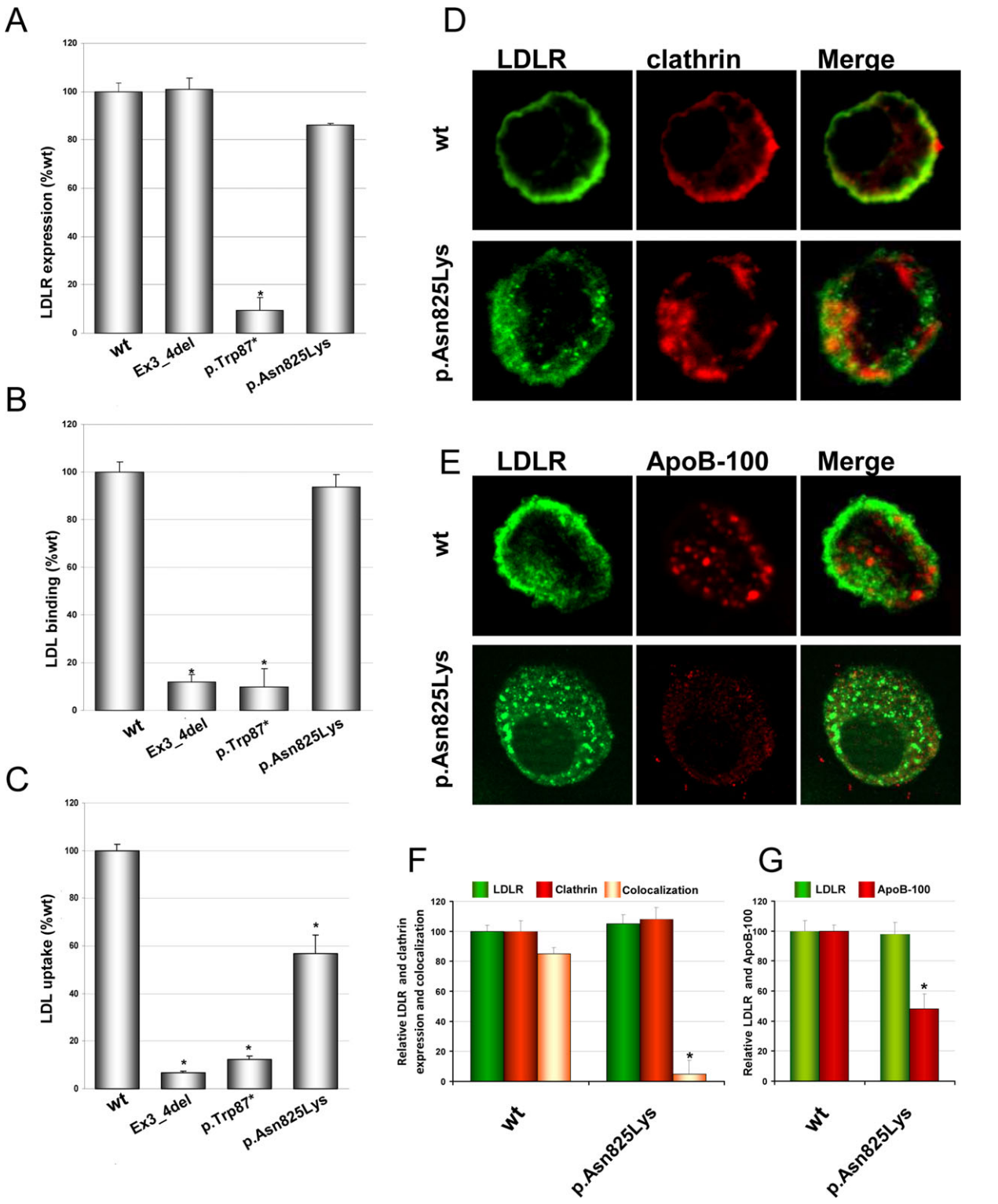

Figure 4. Functional characterization of p.Asn825Lys LDLR variant. Quantification of: **A**: LDLR expression at membrane; **B**: LDL–LDLR binding after 4 hr incubation at 4°C; **C**: LDL internalization after 4 hr at 37°C by FACS; **D**: analysis of colocalization of p.Asn825Lys LDLR variant with clathrin by confocal microscopy; **E**: localization of LDLR and LDL after 4 hr incubation at 37°C; **F**: relative LDLR and clathrin expression and colocalization; and **G**: relative amount of LDLR and LDL. For flow cytometry determinations, 10,000 cells were acquired in a Facscalibur, and values of LDL uptake, binding, and LDLR expression were calculated as described in *Materials and Methods*. Confocal analysis was performed with the transfected cells immunostained as described in *Materials and Methods*. Image analysis to quantify the fluorescence intensities of the confocal images was performed with ImageJ. The values in A–C represent the mean of triplicate determinations ($n = 3$); error bars represent ±SD. $^*P < 0.001$ compared with the wt using a Student's *t*-test. The images in D and E show a representative individual cell. The histograms in F and G represent the mean ± SD ($n = 30$ cells) of the confocal images quantification, $^*P < 0.001$ compared with the wt using a Student's *t*-test.

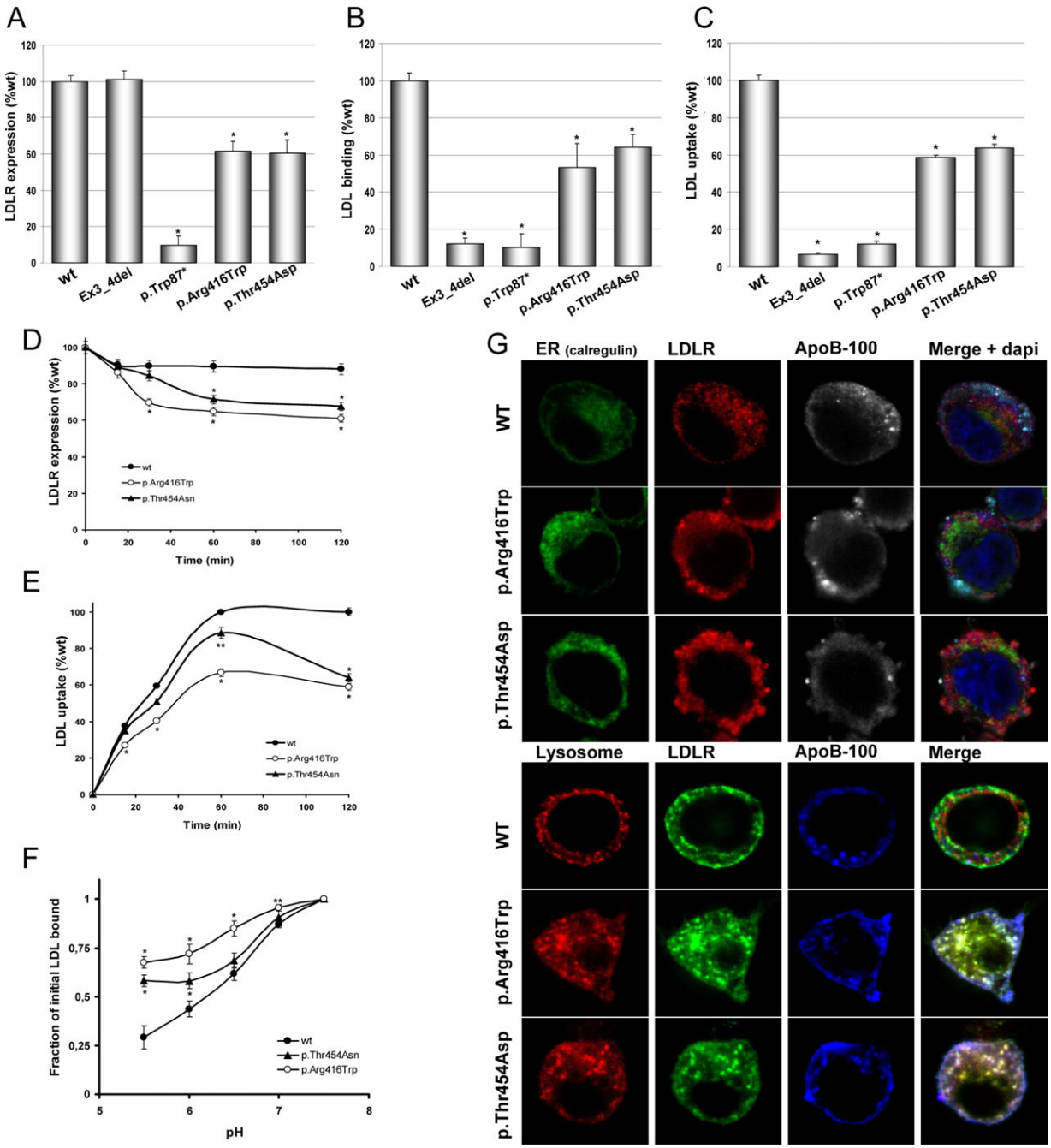

Figure 5. Functional characterization and classification of p.Arg416Thr and p.Thr454Asp LDLR variants. Quantification of: **A**: LDLR expression at membrane; **B**: LDL–LDLR binding after 4 hr incubation at 4°C; **C**: LDL internalization after 4 hr at 37°C by FACS; **D**: kinetics of LDLR expression of wt, p.Arg416Thr, and p.Thr454Asp variants incubated with 20 μg/ml LDL; **E**: kinetics of LDL uptake by cells transfected with wt, p.Arg416Thr or p.Thr454Asp carrying plasmids incubated with 20 μg/ml LDL; **F**: fraction of initial LDL bound to wt, p.Arg416Thr, or p.Thr454Asp variants at different pH. **G**: Subcellular localization of p.Arg416Thr and p.Thr454Asp LDLR variants; upper panel shows colocalization of p.Arg416Thr and p.Thr454Asp LDLR variants with ER and lower panel shows colocalization with lysosomes. For flow cytometry determinations, 10,000 cells were acquired in a Facscalibur, and values of LDL uptake, binding, and LDLR expression were calculated as described in *Materials and Methods*. Expression, uptake, and binding at different pH were determined as described in *Materials and Methods* by FACS. Confocal analysis was performed with the transfected cells immunostained as described in *Materials and Methods*. The values in A–F represent the mean of triplicate determinations ($n = 3$); error bars represent $\pm$SD. $^{**}P < 0.025$; $^{*}P < 0.001$ compared with the wt using a Student's *t*-test. The images in D show a representative individual cell.

internalization resulted diminished in p.Arg416Trp or p.Thr454Asn LDLR variants compared with wt LDLR-transfected cells. To characterize the acid-dependent mechanism of lipoprotein release in the endosomal compartment, we studied LDL–LDLR binding at different pH to mimic the LDL release process occurring in the endosome when the pH is acidified. As shown in Figure 5F, LDL binding was pH dependent for wt, at pH 5.5 LDL binding resulted 75% less efficient compared with that at pH 7.5. In contrast, in p.Arg416Trp and p.Thr454Asn variants, LDL release at acidic pH was not as efficient as in wt. Binding in p.Arg416Trp variant at pH 5.5 diminished 37%

Table 3. Lipid Characteristics of Subjects Carrying Class 2 and Class 5 LDLR Variants Without Statin Treatment and Their Variation (Shown in Percentage) After Statin Treatment

	Class 2 LDLR (p.Ile624del)	Class 5 LDLR (p.Arg416Trp and p.Thr454Asn)	
n	4	12	*P*
Age (year)	41 ± 12.5	46 ± 9.7	0.449
Total cholesterol (mg/dl)	383 ± 56	353 ± 47	0.325
Triglycerides (mg/dl)	64.8 ± 7.8	118 ± 38.6	<0.001
HDL-c (mg/dl)	65.4 ± 2.5	61.7 ± 18.7	0.462
LDL-c (mg/dl)	305 ± 59.5	268.3 ± 41.7	0.253
Apo B (mg/dl)	196.5 ± 9.8	178.6 ± 24.0	0.055
ΔTotal cholesterol (%)	–47.2 ± 6.6	–33.9 ± 13.5	0.010
ΔTriglycerides (%)	–22.8 ± 25.1	–8.9 ± 38.0	0.376
ΔHDL-c (%)	–15.8 ± 14.1	6.1 ± 22.1	0.026
ΔLDL-C (%)	–54.6 ± 8.5	–44.1 ± 16.7	0.090
ΔApo B (%)	–41.1 ± 5.4	–32.1 ± 21.4	0.250

HDL-c, high-density lipoprotein cholesterol; LDL-c, low-density lipoprotein cholesterol; Apo B, apolipoprotein B, Δ, variation.
Data are mean ± SD; *P*, statistical significance for Student's *t*-test.

compared with that at pH 7.5 and binding of LDL to p.Thr454Asn at pH 5.5 was 42% less efficient that at pH 7.5 (Fig. 5F). To confirm that LDLR recycling is defective and that internalized LDLR is degraded in the lysosomes, confocal microscopy analysis of LDLR colocalization in the presence of LDL was conducted. Simultaneously, LDLR localization in the ER was assessed to discard any possible defect on LDLR transport to the cell surface. The images in the upper panel of Figure 5G show no colocalization of LDLR with calregulin, indicating that LDLR transport to the plasma membrane is not defective in these two variants. However, and as expected taking into account the time course LDLR expression, LDL uptake assays, and binding at different pH, LDLR colocalizes with the lysosome marker LAMP-2 both in p.Arg416Trp as in p.Thr454Asn LDLR variant (Fig. 5G, lower panel). The results indicate that p.Arg416Trp and p.Thr454Asn LDLR variants present a defective receptor recycling, thus should be classified as Class 5 pathogenic variants.

Influence of the Class of LDLR Gene Mutation in Response to Statin Therapy

We analyzed the statin response of heterozygous patients carrying p.Ile624del (Class 2) and p.Arg416Trp and p.Thr454Asn (Class 5) variants. Lipid profiles of patients without statin treatment and their variation (shown in percentage) after statin treatment are shown in Table 3. The mean simvastatin dose for Class 2 subjects was 68 ± 39 mg/day and for Class 5 69 ± 45 mg/day during 3 months. Before statin treatment, there were no statistical differences regarding total cholesterol, HDL-c, or LDL-c between patients carrying both Class type variants, although subjects with Class 2 variants carriers showed significantly lower triglyceride levels than Class 5 variant carriers. However, when treated with statins, total cholesterol was significantly diminished in heterozygous patients carrying p.Ile624del Class 2 variant compared with patients carrying p.Arg416Trp and p.Thr454Asn Class 5 variants (–47.2 ± 6.6% vs. –33.9 ± 13.5% decrease, respectively, $P < 0.01$). The LDL-c percentage decrease was also higher in Class 2 compared with Class 5 LDLR variants (–54.6 ± 8.5% vs. –44.1 ± 16.7% decrease, respectively), although without statistical significance. Another difference in statin response of Class 2 and Class 5 LDLR variant patients was that HDL-c levels after treatment in Class 2 subjects decreased and in Class 5 subjects increased, being these differences statistically significant ($P < 0.026$). LDL-c decrease was also determined in patients carrying these variants at different simvastatin doses. The results show that for every simvastatin dose group, the LDL-c percentage decrease was higher for Class 2 LDLR variant patients, although these differences did not reach statistical significance (Supp. Fig. S2).

Discussion

FH is mostly caused by mutations within *LDLR*, which leads to no expression or malfunction of the protein. As a result, clearance of cholesterol-rich LDL particles from circulation decreases, and the elevated blood cholesterol levels cause early onset of atherosclerosis and an increased risk of cardiac disease. LDLR is a modular Class I transmembrane protein that requires a correct folding of its domains for a proper synthesis, trafficking, and function. This process represents a difficult task, partly because of the very high number of intramolecular disulfide bonds present in either the complement-type repeat domains or in the EGF domains and also because calcium incorporation is absolutely necessary for a correct folding. Additionally, packing of the six contiguous YWTD repeats into a six-bladed β-propeller structure may be a very complex process [Springer, 1998; Jeon et al., 2001]. In mammalian cells, LDLR folding occurs in the ER where it is assisted by specialized chaperones [Culi and Mann, 2003; Culi et al., 2004; Sorensen et al., 2006].

Although many FH mutations related to *LDLR* have been identified, most have not yet been classified or functionally characterized. In the current work, we have analyzed and classified seven mutations in the *LDLR* located at different domains of the LDLR.

We have determined that p.Trp577Gly and p.Ile624del variants located in the β-propeller domain are Class 2a variants. Trp577 resides in the fifth YWTD repeat, a structural motif conserved in the EGF domain that defines the β-propeller structure. The six YWTD-tetrapeptide repeats are packed into a six four-stranded beta-sheets ("blades") maintaining the domain structure, which is determinant for a correct folding of β-propeller [Jeon et al., 2001]. In fact, the Trp located in the YWTD repeats, maintains the blade structures by establishing hydrophobic interactions with its surrounding amino acids and also because the indole nitrogen of Trp577 presents a stabilizing hydrogen-bonding interaction with the carboxylate group of the adjacent Asp in the YWTD domain (Fig. 6A). Replacement of Trp577 by a Gly impairs both hydrophobic interactions and hydrogen bonding (Fig. 6B); thus, the protein structure may result in misfolding and failure to exit the ER due to the activity of quality control systems that block the trafficking of misfolded proteins [Ellgaard et al., 1999].

In the case of p.Ile624del variant, the deletion of Ile624 could distort the final conformation of the mature protein by affecting the local environment surrounding the mutation. It is possible that as a result of the advancing in one position of the amino acids after Ile624, the proper interactions among amino acids supporting β-propeller structure are missing.

The third variant also classified as Class 2a is p.Phe800Glyfs*129. This mutation changes the stop codon location and it is predicted to substitute the last 60 amino acids after the membrane domain of the LDLR by a 129 amino acid chain after the membrane domain completely different to wt. It has been shown that residues within the 50 amino acid cytoplasmic domain of the LDLR are involved in the interaction with COPII, a specialized budding machinery that assist trafficking of proteins from the ER to the membrane [Dancourt and Barlowe, 2010]. In addition, it has been described that LDLR lacking the cytoplasmic domain presents a markedly reduced exit from the ER and deletion experiments have shown that at least 30

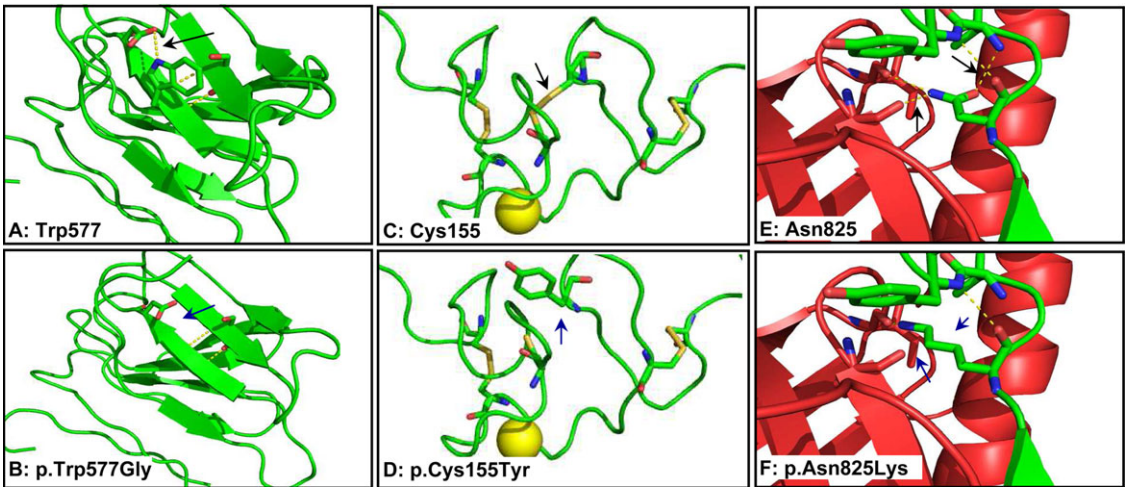

Figure 6. Molecular structures of wt LDLR and p.Trp577Gly, p.Cys155Tyr, and p.Asn825Lys variants. Left panels: Structure of the blades maintained by the Trp located in the YWTD repeats of the β-propeller. **A**: Hydrophobic contacts of the Trp with the surrounding residues, and the water mediated hydrogen bound between the indol group of tryptophan and one carboxylate group of an adjacent Asp maintain the blade structures. **B**: Replacement of Trp577 by a Gly impairs both hydrophobic interactions and hydrogen bonding. Middle panels: Structure of the R4 module of the LDLR-binding domain. **C**: wt structure representing the two main structural motifs of the module, three disulfide bonds, and Ca^{2+} coordination, allowing a correct LDLR conformation for LDL binding. **D**: Tyr at 155 position disrupts one of the disulfide bond between cystein 155 and 173. Right panel: Structure of the LDLRAP1 (in red) and the LDLR cytoplasmic tail (in green) interaction. **E**: Asn825 maintains the Hook-like structure of the LDLR cytoplasmic tail by the interaction with Val and Tyr of the FxNPxY, and binds LDLRAP1 with its NH_2 by polar contacts with Ile115 and Ile112. **F**: Replacement of Asn825 by a Lys impairs the polar contact with the amide backbone of Val827 and due to its difference in size it cannot bind with the same efficiency the two Ile. This figure was prepared with PyMOL (DeLano Scientifics) (PDB:1N7D) (PDB:3S06).

residues of the cytoplasmic domain have to be present for the LDLR to efficiently exit the ER [Strom et al., 2011]. Hence, being the length of the cytoplasmic domain a key determinant for exiting from the ER, it is reasonable to assume that the modified LDLR sequence is not recognized resulting in protein ER retention. In addition, this mutation lacks functionally important motifs of the cytoplasmic domain involved in the internalization, FxNPxY motif [Chen et al., 1990], and the signal for basolateral sorting located within residues 812–828 [Yokode et al., 1992].

We have also classified p.Cys155Tyr variant, located in the LDLR–LDL-binding domain as Class 3 pathogenic variant. The LDLR–LDL-binding domain harbors seven cysteine-rich repeats that stabilize its structure by three disulfide bonds (Fig. 6C) that maintain a correct LDLR conformation for LDL binding [Fass et al., 1997]. Cys155 is absolutely required to establish a disulfide bond. Hence, Cys replacement by a Tyr in position 155 abolishes the disulfide bond between Cys155 and Cys173 (Fig. 6D). In consequence, the required compact structure that forms patches of conserved acidic residues within the surface of the R modules is missing. Nevertheless, the conformational change seems not to be enough to be retained in the ER as the Class 2 mutations; LDLR reaches the membrane but is not able to bind LDL.

The characterization of p.Asn825Lys shows that replacement of Asn by Lys in the FxNPxY motif results pathogenic. LDLR–clathrin-mediated endocytosis depends on the LDL receptor adaptor protein 1 (LDLRAP1), which binds the LDLR cytoplasmic tail at its FxNPxY internalization signal and serves as an adaptor protein interacting with clathrin. It has been shown that FxNPxY sequence assumes a unique "Hook"-like structure with a double β-turn conformation, maintained by the interaction between the Asn825 backbone carboxylate and Tyr828 backbone amide groups, and also because the carboxylate oxygen atom of the Asn825 side chain establishes an hydrogen bond with the backbone amide group of Val827 [Dvir et al., 2012] (Fig. 6E). The interaction of FxNPxY motif with the autosomal-recessive hypercholesterolemia (LDLRAP1) protein is mediated by the NH_2 group of Asn825 that establishes polar contacts with the backbone carboxylate groups of Ile115 and Ile112. In addition to these interactions, this β-turn allows accommodation of Tyr828 of the FxNPxY in a hydrophobic groove of the surface of LDLRAP1. As shown in Figure 6F, substitution of Asn825 by a Lys impairs the contact between Asn825 and Val827 that helps in the β-turn stabilization. Even though NH_2 group of Lys could interact with Ile115 and Ile112 of LDLRAP1 in a similar way than Asn, it seems that differences in size and space orientation of both amino acids may hinder the polar contacts established by Lys 825 with Ile115 and Ile112 and allow, at the same time, the insertion of Tyr828 in the hydrophobic groove of LDLRAP1.

p.Arg416Trp and p.Thr454Asn variants, both located on the β-propeller, have been classified as Class 5. LDLR Class 5 variants result in mutant receptors that fail to release LDL in the sorting endosome. As a consequence, LDLRs are directed to the lysosomes for degradation rather than being recycled [Beglova et al., 2004; Van Hoof et al., 2005]. It is well established that at the mildly acidic pH of the sorting endosomes, the LDLR undergoes a conformational change whereby the ligand-binding domain folds back on the β-propeller of the EGF precursor homology domain [Rudenko et al., 2002]. The LDLR thus adopts a closed conformation and LDL is released from the LDLR. While released LDL is transported to the lysosomes for degradation, the LDLR is recycled back to the cell membrane [Davis et al., 1987]. The majority of Class 5 mutations reside in exons-encoding residues of the EGF precursor homology domain that is critical for the normal recycling of the LDLR [Hobbs et al., 1992]. It is well established as to which are the residues implicated in the interaction between LR4 and LR5 in the binding domain, and β-propeller in EGF-like domain to get the closed conformation of the LDLR at acidic pH necessary for a proper back of the receptor to the plasma membrane [Rudenko et al., 2002]. But there are many other variants like p.Arg416Trp and p.Thr454Asn, located out of this region of the

β-propeller belonging to Class 5 [Hobbs et al., 1992]. The incorrect pH-dependent dissociation corroborated for p.Arg416Trp and p.Thr454Asn variants would indicate that the β-propeller may be more flexible, and in the conformational rearrangements occurring in the endosome, there could be involved more changes than the expected to date.

The clinical phenotype of FH patients is highly variable, and there is also a considerable interindividual variation in their response to lipid-lowering treatment, and several genetic and environmental factors can contribute to this variability. It has been suggested that the class of the *LDLR* mutation could affect the LDL-c- and apoB-lowering response of heterozygous FH patients to statin therapy [Leren and Hjermann, 1995; Vuorio et al., 1995]. To date, some studies addressing this question have been performed, and so far they are not conclusive but controversial [Choumerianou and Dedoussis, 2005]. In this study, we have found that lipid phenotype of heterozygous patients carrying p.Ile624del Class 2 variant is similar to the p.Arg416Trp and p.Thr454Asn Class 5 variants. However, subjects with Class 2 LDLR variants showed a higher reduction in lipid levels after statin treatment than subjects with Class 5 LDLR variants, both taking into account all subjects with different simvastatin doses together, as grouped by milligram of simvastatin, ranging from 20 to 120 mg/day. This is in contraposition with other previous studies that found the opposite [Miltiadous et al., 2006]. However, in view of the limited number of patients included in this study, additional studies with higher sample number and different classes of LDLR variants are required to demonstrate a differential effect of simvastatin. These controversial results highlight the importance of pharmacogenomic research on existing drugs, such as statins, to improve the efficacy or safety of therapy. The in vitro studies performed with these LDLR variants clearly show that in the homozygous situation Class 2 and Class 3 variants result in a more severe phenotype than Class 4 and Class 5 variants. This could be explained because in the Class 4 and Class 5 heterozygote states, both wt and mutant LDLR are expressed on the cell surface. Since in defective Class 4 and Class 5 types, the receptor maintains its function (binding in Class 4 or binding and internalization in Class 5), some LDL is cleared by these receptors, contributing somehow to total LDLR activity in these patients.

Conclusion

The present work highlights the importance of functional characterization of LDLR variants to provide an indisputable diagnosis of FH, particularly in children for which the clinical diagnosis can be difficult. In addition, the combined methodology used in this study allows classification of *LDLR* variants providing information that benefit the understanding of FH and could help predict the effect of a mutation in LDLR function, at least in the homozygous state. Very interesting, although not conclusive, is the different response to statins observed in patients carrying Class 2 or Class 5 variants but additional experiments should be performed to confirm these results.

Acknowledgments

Technical and human support provided by SGIker (Analytical and High-Resolution Microscopy in Biomedicine Service of the UPV/EHU) and Rocío Alonso for excellent technical assistance are gratefully acknowledged. We thank Prof. A. Gómez-Muñoz for flow cytometry facilities, Dr. Patricia Villacé for kindly providing clathrin-DsRed plasmid, and Dr. Monty Krieger for kindly providing *CHO-ldlA7* cells.

References

Abifadel M, Varret M, Rabes JP, Allard D, Ouguerram K, Devillers M, Cruaud C, Benjannet S, Wickham L, Erlich D, Derré A, Villéger L, et al. 2003. Mutations in PCSK9 cause autosomal dominant hypercholesterolemia. Nat Genet 34:154–156.

Beglova N, Jeon H, Fisher C, Blacklow SC. 2004. Cooperation between fixed and low pH-inducible interfaces controls lipoprotein release by the LDL receptor. Mol Cell 16:281–292.

Bertolini S, Pisciotta L, Rabacchi C, Cefalu AB, Noto D, Fasano T, Signori A, Fresa R, Averna M, Calandra S. 2013. Spectrum of mutations and phenotypic expression in patients with autosomal dominant hypercholesterolemia identified in Italy. Atherosclerosis 227:342–348.

Brown MS, Goldstein JL. 1986. A receptor-mediated pathway for cholesterol homeostasis. Science 232:34–47.

Culi J, Mann RS. 2003. Boca, an endoplasmic reticulum protein required for wingless signaling and trafficking of LDL receptor family members in Drosophila. Cell 112:343–354.

Culi J, Springer TA, Mann RS. 2004. Boca-dependent maturation of beta-propeller/EGF modules in low-density lipoprotein receptor proteins. EMBO J 23:1372–1380.

Chaves FJ, Real JT, Garcia-Garcia AB, Civera M, Armengod ME, Ascaso JF, Carmena R. 2001. Genetic diagnosis of familial hypercholesterolemia in a South European outbreed population: influence of low-density lipoprotein (LDL) receptor gene mutations on treatment response to simvastatin in total, LDL, and high-density lipoprotein cholesterol. J Clin Endocrinol Metab 86:4926–4932.

Chen WJ, Goldstein JL, Brown MS. 1990. NPXY, a sequence often found in cytoplasmic tails, is required for coated pit-mediated internalization of the low density lipoprotein receptor. J Biol Chem 265:3116–3123.

Chmara M, Wasag B, Zuk M, Kubalska J, Wegrzyn A, Bednarska-Makaruk M, Pronicka E, Wehr H, Defesche JC, Rynkiewicz A, Limon J. 2010. Molecular characterization of Polish patients with familial hypercholesterolemia: novel and recurrent LDLR mutations. J Appl Genet 51:95–106.

Choumerianou DM, Dedoussis GV. 2005. Familial hypercholesterolemia and response to statin therapy according to LDLR genetic background. Clin Chem Lab Med 43:793–801.

Dancourt J, Barlowe C. 2010. Protein sorting receptors in the early secretory pathway. Annu Rev Biochem 79:777–802.

Davis CG, Goldstein JL, Sudhof TC, Anderson RG, Russell DW, Brown MS. 1987. Acid-dependent ligand dissociation and recycling of LDL receptor mediated by growth factor homology region. Nature 326:760–765.

Davis CG, Lehrman MA, Russell DW, Anderson RG, Brown MS, Goldstein JL. 1986. The J.D. mutation in familial hypercholesterolemia: amino acid substitution in cytoplasmic domain impedes internalization of LDL receptors. Cell 45:15–24.

Dvir H, Shah M, Girardi E, Guo L, Farquhar MG, Zajonc DM. 2012. Atomic structure of the autosomal recessive hypercholesterolemia phosphotyrosine-binding domain in complex with the LDL-receptor tail. Proc Natl Acad Sci USA 109:6916–6921.

Ellgaard L, Molinari M, Helenius A. 1999. Setting the standards: quality control in the secretory pathway. Science 286:1882–1888.

Etxebarria A, Palacios L, Stef M, Tejedor D, Uribe KB, Oleaga A, Irigoyen L, Torres B, Ostolaza H, Martin C. 2012. Functional characterization of splicing and ligand-binding domain variants in the LDL receptor. Hum Mutat 33:232–243.

Fass D, Blacklow S, Kim PS, Berger JM. 1997. Molecular basis of familial hypercholesterolaemia from structure of LDL receptor module. Nature 388:691–693.

Goldstein JL, Brown MS. 2001. *Familial hypercholesterolemia*. New York: McGraw-Hill.

Gudnason V, Humphries SE. 1999. Hyperhomocysteinaemia, genetics and cardiovascular disease risk. Eur Heart J 20:552–523.

Hobbs HH, Brown MS, Goldstein JL. 1992. Molecular genetics of the LDL receptor gene in familial hypercholesterolemia. Hum Mutat 1:445–466.

Hoeg JM. 1993. Homozygous familial hypercholesterolemia: a paradigm for phenotypic variation. Am J Cardiol 72:11D–14D.

Holla OL, Kulseth MA, Berge KE, Leren TP, Ranheim T. 2009. Nonsense-mediated decay of human LDL receptor mRNA. Scand J Clin Lab Invest 69:409–417.

Innerarity TL, Mahley RW, Weisgraber KH, Bersot TP, Krauss RM, Vega GL, Grundy SM, Friedl W, Davignon J, McCarthy BJ. 1990. Familial defective apolipoprotein B-100: a mutation of apolipoprotein B that causes hypercholesterolemia. J Lipid Res 31:1337–1349.

Jensen JM, Kruse TA, Brorholt-Petersen JU, Christiansen TM, Jensen HK, Kolvraa S, Faergeman O. 1999. Linking genotype to aorto-coronary atherosclerosis: a model using familial hypercholesterolemia and aorto-coronary calcification. Ann Hum Genet 63(Pt 6):511–520.

Jeon H, Meng W, Takagi J, Eck MJ, Springer TA, Blacklow SC. 2001. Implications for familial hypercholesterolemia from the structure of the LDL receptor YWTD-EGF domain pair. Nat Struct Biol 8:499–504.

Kotze MJ, Davis HJ, Bissbort S, Langenhoven E, Brusnicky J, Oosthuizen CJ. 1993. Intrafamilial variability in the clinical expression of familial hypercholesterolemia: importance of risk factor determination for genetic counselling. Clin Genet 43:295–299.

Leigh SE, Foster AH, Whittall RA, Hubbart CS, Humphries SE. 2008. Update and analysis of the University College London low density lipoprotein receptor familial hypercholesterolemia database. Ann Hum Genet 72(Pt 4):485–498.

Leren TP, Hjermann I. 1995. Is responsiveness to lovastatin in familial hypercholesterolaemia heterozygotes influenced by the specific mutation in the low-density lipoprotein receptor gene? Eur J Clin Invest 25:967–973.

Leren TP, Tonstad S, Gundersen KE, Bakken KS, Rodningen OK, Sundvold H, Ose L, Berg K. 1997. Molecular genetics of familial hypercholesterolaemia in Norway. J Intern Med 241:185–194.

Marduel M, Carrie A, Sassolas A, Devillers M, Carreau V, Di Filippo M, Erlich D, Abifadel M, Marques-Pinheiro A, Munnich A, Junien C; French ADH Research Network, et al. 2010. Molecular spectrum of autosomal dominant hypercholesterolemia in France. Hum Mutat 31:E1811–E1824.

Miltiadous G, Saougos V, Cariolou M, Elisaf MS. 2006. Plasma lipoprotein(a) levels and LDL-cholesterol lowering response to statin therapy in patients with heterozygous familial hypercholesterolemia. Ann Clin Lab Sci 36:353–355.

Mozas P, Castillo S, Tejedor D, Reyes G, Alonso R, Franco M, Saenz P, Fuentes F, Almagro F, Mata P, Pocoví M. 2004. Molecular characterization of familial hypercholesterolemia in Spain: identification of 39 novel and 77 recurrent mutations in LDLR. Hum Mutat 24:187.

Palacios L, Grandoso L, Cuevas N, Olano-Martin E, Martinez A, Tejedor D, Stef M. 2012. Molecular characterization of familial hypercholesterolemia in Spain. Atherosclerosis 221:137–142.

Rudenko G, Henry L, Henderson K, Ichtchenko K, Brown MS, Goldstein JL, Deisenhofer J. 2002. Structure of the LDL receptor extracellular domain at endosomal pH. Science 298:2353–2358.

Sorensen S, Ranheim T, Bakken KS, Leren TP, Kulseth MA. 2006. Retention of mutant low density lipoprotein receptor in endoplasmic reticulum (ER) leads to ER stress. J Biol Chem 281:468–476.

Soutar AK, Naoumova RP. 2007. Mechanisms of disease: genetic causes of familial hypercholesterolemia. Nat Clin Pract Cardiovasc Med 4:214–225.

Springer TA. 1998. An extracellular beta-propeller module predicted in lipoprotein and scavenger receptors, tyrosine kinases, epidermal growth factor precursor, and extracellular matrix components. J Mol Biol 283:837–862.

Strom TB, Tveten K, Holla OL, Cameron J, Berge KE, Leren TP. 2011. Characterization of residues in the cytoplasmic domain of the LDL receptor required for exit from the endoplasmic reticulum. Biochem Biophys Res Commun 415:642–645.

Sudhof TC, Goldstein JL, Brown MS, Russell DW. 1985. The LDL receptor gene: a mosaic of exons shared with different proteins. Science 228:815–822.

Tolleshaug H, Goldstein JL, Schneider WJ, Brown MS. 1982. Posttranslational processing of the LDL receptor and its genetic disruption in familial hypercholesterolemia. Cell 30:715–724.

Tosi I, Toledo-Leiva P, Neuwirth C, Naoumova RP, Soutar AK. 2007. Genetic defects causing familial hypercholesterolaemia: identification of deletions and duplications in the LDL-receptor gene and summary of all mutations found in patients attending the Hammersmith Hospital Lipid Clinic. Atherosclerosis 194:102–111.

Van Hoof D, Rodenburg KW, Van der Horst DJ. 2005. Intracellular fate of LDL receptor family members depends on the cooperation between their ligand-binding and EGF domains. J Cell Sci 118(Pt 6):1309–1320.

Vohl MC, Szots F, Lelievre M, Lupien PJ, Bergeron J, Gagne C, Couture P. 2002. Influence of LDL receptor gene mutation and apo E polymorphism on lipoprotein response to simvastatin treatment among adolescents with heterozygous familial hypercholesterolemia. Atherosclerosis 160:361–368.

Vuorio AF, Ojala JP, Sarna S, Turtola H, Tikkanen MJ, Kontula K. 1995. Heterozygous familial hypercholesterolaemia: the influence of the mutation type of the low-density-lipoprotein receptor gene and PvuII polymorphism of the normal allele on serum lipid levels and response to lovastatin treatment. J Intern Med 237:43–48.

Yamamoto T, Davis CG, Brown MS, Schneider WJ, Casey ML, Goldstein JL, Russell DW. 1984. The human LDL receptor: a cysteine-rich protein with multiple Alu sequences in its mRNA. Cell 39:27–38.

Yokode M, Pathak RK, Hammer RE, Brown MS, Goldstein JL, Anderson RG. 1992. Cytoplasmic sequence required for basolateral targeting of LDL receptor in livers of transgenic mice. J Cell Biol 117:39–46.